Journal of Dental Sciences 20 (2025) 393–401

Available online at www.sciencedirect.com

ScienceDirect

journal homepage: www.e-jds.com

Original Article

Automatic classification of temporomandibular joint disorders by magnetic resonance imaging and convolutional neural networks

Ting-Yi Su [a†], Jacky Chung-Hao Wu [a†], Wen-Chi Chiu [b,c,d], Tzeng-Ji Chen [b,c,e], Wen-Liang Lo [f,g**], Henry Horng-Shing Lu [a,h*]

[a] *Institute of Statistics, National Yang Ming Chiao Tung University, Hsinchu City, Taiwan*
[b] *Department of Family Medicine, Taipei Veterans General Hospital, Taipei City, Taiwan*
[c] *Big Data Center, Department of Medical Research, Taipei Veterans General Hospital, Taipei City, Taiwan*
[d] *Institute of Artificial Intelligence Innovation, National Yang Ming Chiao Tung University, Hsinchu City, Taiwan*
[e] *Department of Family Medicine, Taipei Veterans General Hospital Hsinchu Branch, Hsinchu County, Taiwan*
[f] *Section of Oral and Maxillofacial Surgery, Department of Stomatology, Taipei Veterans General Hospital, Taipei City, Taiwan*
[g] *Department of Dentistry, College of Dentistry, National Yang Ming Chiao Tung University, Taipei City, Taiwan*
[h] *Department of Statistics and Data Science, Cornell University, Ithaca, NY, USA*

Received 9 May 2024; Final revision received 3 June 2024
Available online 15 June 2024

KEYWORDS
Convolutional neural network;
Machine learning;
Temporomandibular joint disorders

Abstract *Background/purpose:* In this study, we utilized magnetic resonance imaging data of the temporomandibular joint, collected from the Division of Oral and Maxillofacial Surgery at Taipei Veterans General Hospital. Our research focuses on the classification and severity analysis of temporomandibular joint disease using convolutional neural networks.
Materials and methods: In gray-scale image series, the most critical features often lie within the articular disc cartilage, situated at the junction of the temporal bone and the condyles. To

* Corresponding author. Institute of Statistics, National Yang Ming Chiao Tung University, No. 1001, Daxue Rd., East Dist., Hsinchu City 300093 Taiwan.
** Corresponding author. Section of Oral and Maxillofacial Surgery, Department of Stomatology, Taipei Veterans General Hospital, No. 201, Sec. 2, Shipai Rd., Beitou Dist., Taipei City 11217 Taiwan.
E-mail addresses: wllo@vghtpe.gov.tw (W.-L. Lo), henryhslu@nycu.edu.tw (H.H.-S. Lu).
† These authors contributed equally to this work.

https://doi.org/10.1016/j.jds.2024.06.001

identify this region efficiently, we harnessed the power of You Only Look Once deep learning technology. This technology allowed us to pinpoint and crop the articular disc cartilage area. Subsequently, we processed the image by converting it into the HSV format, eliminating surrounding noise, and storing essential image information in the V value. To simplify age and left-right ear information, we employed linear discriminant analysis and condensed this data into the S and H values.

Results: We developed the convolutional neural network with six categories to identify severe stages in patients with temporomandibular joint (TMJ) disease. Our model achieved an impressive prediction accuracy of 84.73%.

Conclusion: This technology has the potential to significantly reduce the time required for clinical imaging diagnosis, ultimately improving the quality of patient care. Furthermore, it can aid clinical specialists by automating the identification of TMJ disorders.

Introduction

The temporomandibular joint (TMJ) is situated between the temporal bone and the mandibular condyles, located near the left and right ears.[1] Clinically, TMJD is divided into five stages according to severity. Different stages of TMJD will also be reflected in images. The first stage causes a subtle sound when opening the mouth, which is usually undetectable. The second stage is the inflammatory stage. Dislocation of cartilage can be seen on imaging, causing pain in inflammatory diseases. In the third stage, although the inflammation subsides, changes in the shape of the cartilage can be seen in images. In the fourth stage, the pain shifts to the muscles over the temporomandibular joint. In the fifth stage, the pain extends to the head and affects daily life, requiring immediate surgery.

Research in the field of TMJ encompasses both anatomy and biomechanics.[2] One of the most prevalent symptoms of temporomandibular joint disorder (TMJD) is the anterior movement of the articular cartilage against the condyle when the mouth is opened and closed.[3] This condition, diagnosed in 41% of TMJD cases, often leads to pain and inflammation in affected patients.[4] Additionally, 33% of individuals experience disc displacement with reduction (DDWR), which may or may not present with symptoms and may necessitate further diagnosis through imaging.[5]

According to data, temporomandibular joint disorders (TMJD) afflict approximately 5—15% of the population, with a higher prevalence among females compared to males. The treatment of TMJ typically spans duration of 3—6 months, and each consultation and diagnosis can be time-intensive. Due to the potential overlap of TMJD symptoms with other joint conditions, diagnosing TMJD presents a significant challenge for dentists. Early detection and prompt treatment are crucial for patients' recovery after surgery.[6] In the realm of medical imaging, magnetic resonance imaging (MRI) stands out as a superior choice. It offers clearer and more detailed information, serving as a vital foundation for diagnosing the stage of TMJD.[7]

Traditionally, in establishing automatic identification of TMJ images, in addition to image segmentation, image augmentation, and training CNN models,[8,9] we were inspired. In addition to using the above methods, we using the You Only Look Once (YOLO) model to remain the articular disc cartilage area, and subjects' age information are used for image coloring, and finally a Convolutional Neural Networks (CNNs) model is established to automatically identify the five TMJ stages.

Convolutional Neural Networks (CNNs), drawing inspiration from natural visual perception and biological mechanisms, stand as a well-established deep learning model. The widespread adoption of deep learning in the medical field, including oral and maxillofacial surgery, has paved the way for transformative advancements. Deep learning methods diverge from traditional statistical approaches found in software packages, which rely on distribution calculations based on mean and standard deviation. Utilizing the power of CNNs, we've developed a trained model capable of classifying various states of Temporomandibular Joint Disorder (TMJD). This innovative approach aids clinicians in diagnosing the severity of TMJD through medical imaging, facilitating early symptom detection, and reducing consultation time. This fusion of advanced technology and medical expertise holds immense promise for enhancing patient care.

Materials and methods

Data introduction

The study population consisted of magnetic resonance imaging (MRI) images from 194 patients, which were collected in the Division of Oral and Maxillofacial Surgery at Taipei Veterans General Hospital, Taipei City, Taiwan, between 2009 and 2021. This study received approval from the ethics committee at Taipei Veterans General Hospital (IRB number: 2018-07-051BC).

In this study, mouth-opening images sized at 512 $\times$ 512 pixels were utilized. Each participant contributed thirty-two images, comprising cross-sections extending from the right ear to the left ear. In clinical diagnosis, the stage of Temporomandibular Joint Disorder (TMJD) is assessed based on the extent of articular cartilage disc displacement.

In our image preprocessing pipeline, we initially removed noise by cropping the surrounding organs, following the techniques outlined.[10,11] Subsequently, we employed object detection methods to identify and isolate the articular cartilage disc area. To ensure uniformity, all images were padded and resized to the same dimensions. A unique touch was added to the image processing by incorporating subjects' age information into the image color. These preprocessed images were then fed into our Convolutional Neural Network (CNN) model for analysis. A visual representation of the image preprocessing steps can be found in Fig. 1.

Cropping

In contemporary deep learning, the You Only Look Once (YOLO) method has become a prominent choice for object detection.[12] YOLO comprises three key processes: object localization, feature extraction, and image classification, all performed seamlessly through Convolutional Neural Networks (CNNs).[13] Our study specifically adopts YOLO version 3 due to its utilization of an improved CNN model compared to other YOLO variants. This version incorporates multidimensional prediction and employs a binary entropy loss function, resulting in enhanced prediction accuracy.[14]

To begin, we marked the articular cartilage disc area within our dataset, which comprised a total of 2005 images from 194 participants. These images were randomly divided into two sets: 1644 for training and 361 for testing. During training, all layers of the YOLO model were unlocked, and the training process continued until early stopping criteria were met. The loss curves for both the training and test sets demonstrated a gradual decrease, as depicted in Fig. 2, eventually reaching a satisfactory level below 5. To assess the performance of our YOLO model, we utilized Intersection over Union (IoU). The average IoU value for the test images was calculated at 0.7409. In Fig. 3, the blue frame represents the actual object frame, while the red frame signifies the predicted object frame generated by the YOLO model. These predicted object frames were employed for image cropping.

Given the nature of our dataset, which consists of cross-sectional images spanning from the right ear to the left ear, the temporomandibular joint and its symptomatic areas may not always appear in every image. Consequently, if no predicted bounding box is generated, it is reasonable to exclude the image from further analysis. For each subject, we selected the top three images with the largest predicted frame areas for subsequent processing. However, all images put into the CNN model come from the test set of the YOLO model, and the selected images are determined by the prediction results of the YOLO model. This is a passive selection, not a manual selection. Data manipulation does not exist.

To address differences in the extent of predicted object frames and selected images across participants, we employed a solution involving resizing and padding.[15,16] Initially, we symmetrically padded the cropped rectangular images with black edges to create square images. Subsequently, we resized them to a uniform dimension of 112 pixels × 112 pixels. The outcome of this process is illustrated in Fig. 4.

Image colorization

Age, gender, and race may influence the determination of TMJD stage, and our original data set included out-of-image effects of age. Research has demonstrated that colorizing gray-scale images can enhance visualization, improve interpretability, assist feature extraction, and enhance prediction accuracy.[17] In our approach, we read gray-scale images in the HSV color format, with image intensity information stored in the Value component. After cropping, we incorporated the subject's age information and created a dummy variable to encode left-right ear image information as 0 or 1. Linear discriminant analysis (LDA) was then applied to reduce the age and left-right ear information to two dimensions, which were stored as Saturation and Hue values. The reference category for LDA dimensionality reduction was the TMJ stage. Finally, we converted the images back into RGB format before feeding them into the CNN model. The image colorization results can be observed in Fig. 5. The LDA method does not target image information (value component), which avoids the loss of image information, and only targets training sets, which avoids the introduction of bias.

Model prediction

After completing the image preprocessing step, we recognized the need to augment our dataset due to its limited size. Data augmentation can be based on the original image by fine-tuning or synthesizing more simulated images. The main purpose is to prevent over-fitting. It is especially effective for training with a small amount of data and can improve the accuracy of the model. To increase the volume of training data, we applied data augmentation, effectively expanding it by a factor of 8. This augmentation was executed using the 'ImageDataGenerator' package in our Python program, which generates new images through random rotations and translations. The specific parameters used for data augmentation were as follows: Rotation range. Randomly choose forward or reverse rotation within

Figure 1 Image preprocessing steps containing you only look once (yolo) cropping model, filling black border and scaling to unify size, image coloring.

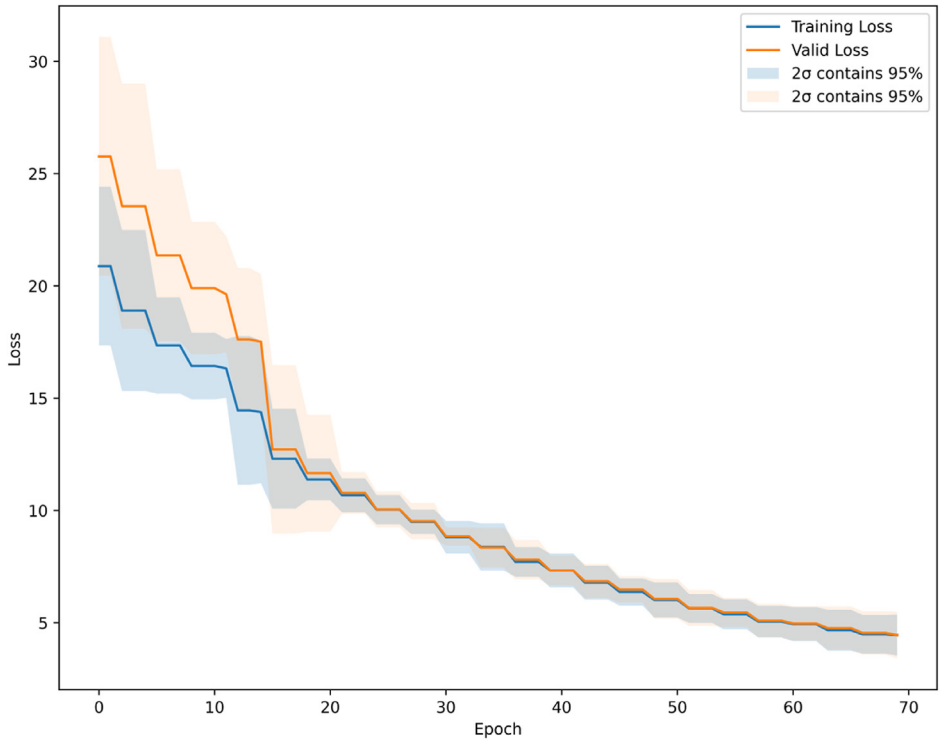

Figure 2 You only look once (YOLO) training loss curve. This graph displays the training loss curve for the YOLO model during training iterations, allowing for an assessment of model convergence.

20° based on the center point; Width shift range. Randomly shift within 10% of the image width left and right; Height shift range. Randomly shift within 10% of the image height up and down. The augmentation results, highlighting the increased diversity of our dataset, can be observed in Fig. 6.

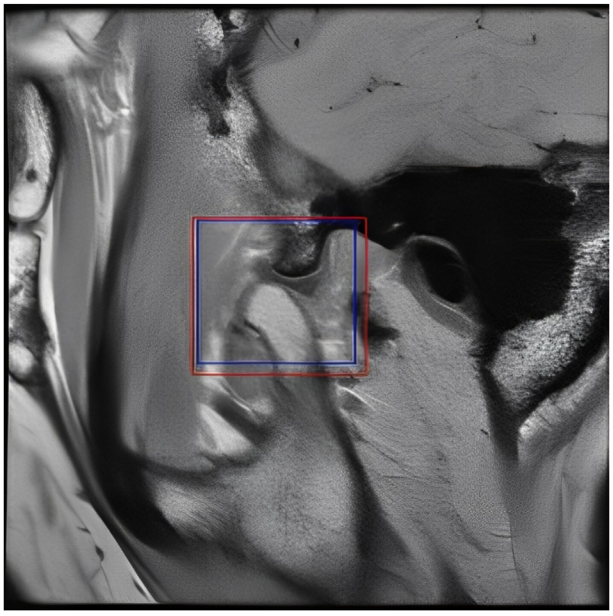

Figure 3 You only look once (YOLO) testing bounding boxes which show the predicted region of the YOLO model (red box) and the corresponding real region (blue box). (For interpretation of the references to color in this figure legend, the reader is referred to the Web version of this article.)

Following data augmentation, we evenly distributed the augmented data into training and test sets based on the TMJD stage. The data proportions are summarized in Table 1.

Optimal model hyper-parameters

In the realm of deep learning, CNN models have proven effective for image classification tasks. These models can capture image similarities, extract features using a relatively small number of model parameters, thus reducing training time and addressing memory constraints. Hence, our study employs a CNN model, specifically the VGG16 architecture.

To mitigate over-fitting, we modified the model by updating a fully connected layer at the bottom and incorporating dropout regularization. The model architecture is visualized in Fig. 7. We employed transfer learning, initializing our model with pre-trained weights from the ImageNet image set.

During the hyper-parameter tuning stage, we focused on tuning factors related to the number of pre-training layers with fixed weight values from the top. The remaining convolutional layer weights were updated during training. We adopted a five-fold cross-validation approach for hyper-parameter tuning,[18,19] computing the average accuracy across the five folds and selecting the hyper-parameters corresponding to the highest accuracy value. Finally, we used both the training and validation images to predict the results of the test set, ensuring robust model evaluation.

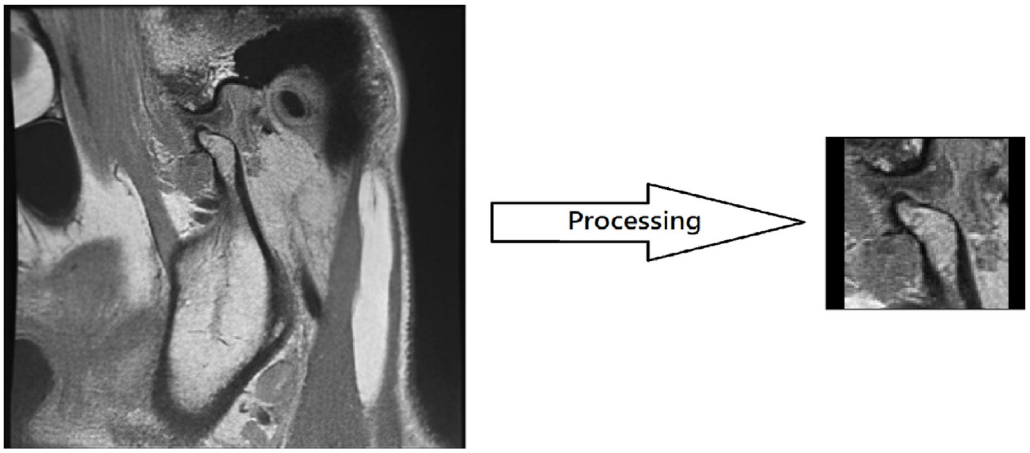

Figure 4 Image processing result. This image provides a direct comparison of the image before and after the image processing steps. It illustrates the visual effects and improvements achieved through the preprocessing procedures applied to the image.

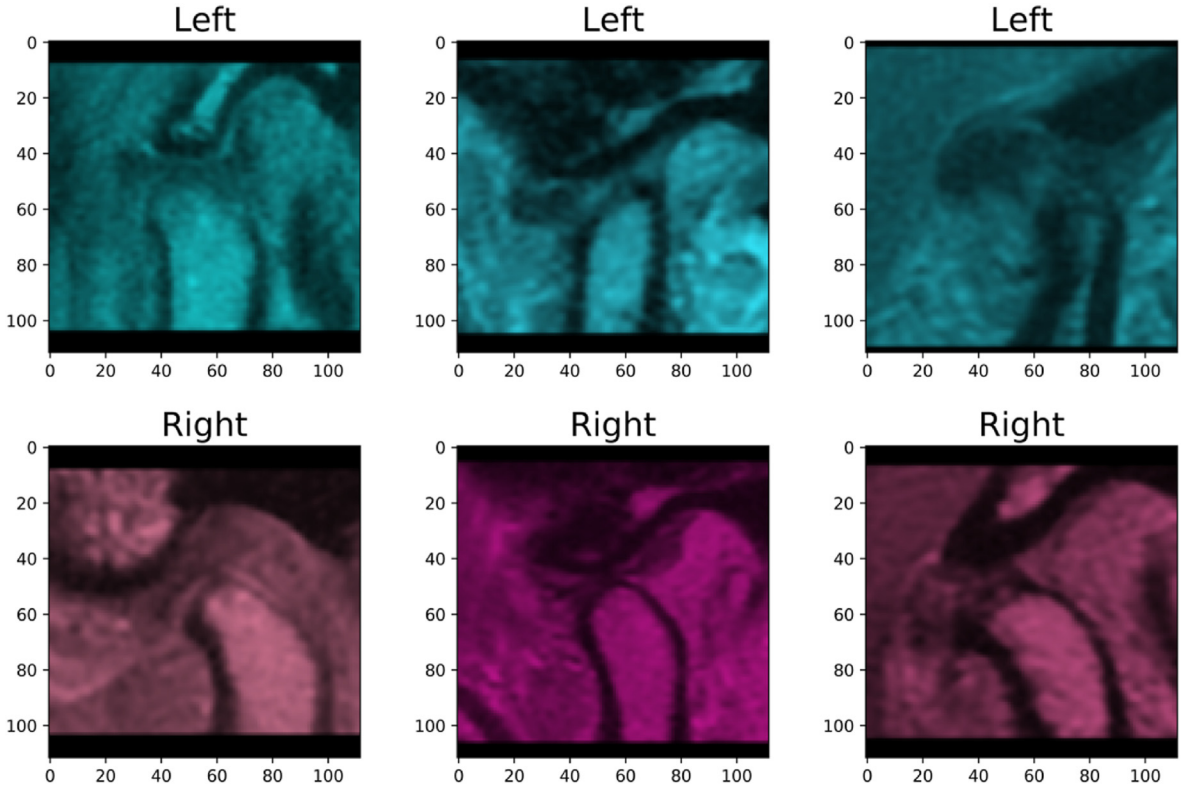

Figure 5 Image colorization result. This figure showcases the outcomes of image colorization for both the left ear and the right ear, obtained from different subjects. It visually demonstrates the effects of applying color to gray-scale images, enhancing their interpretability and visualization. (For interpretation of the references to color in this figure legend, the reader is referred to the Web version of this article.)

Results

The results of hyper-parameter tuning, summarized in Table 2, revealed that the optimal number of pre-training weight layers is 3.

As part of our model evaluation process utilizing the five-fold cross-validation method, we generated five sets of loss and accuracy curves, as depicted in Fig. 8. These curves demonstrated a consistent and steady decrease in loss over epochs. Importantly, the small variance between the curves indicated minimal deviation in the five validation results. Eventually, the loss value stabilized below 1.5, reaching a reasonable and stable level, while the accuracy curve exhibited steady improvement.

We conducted a performance evaluation on the test set, where prediction results were calculated on a per-subject

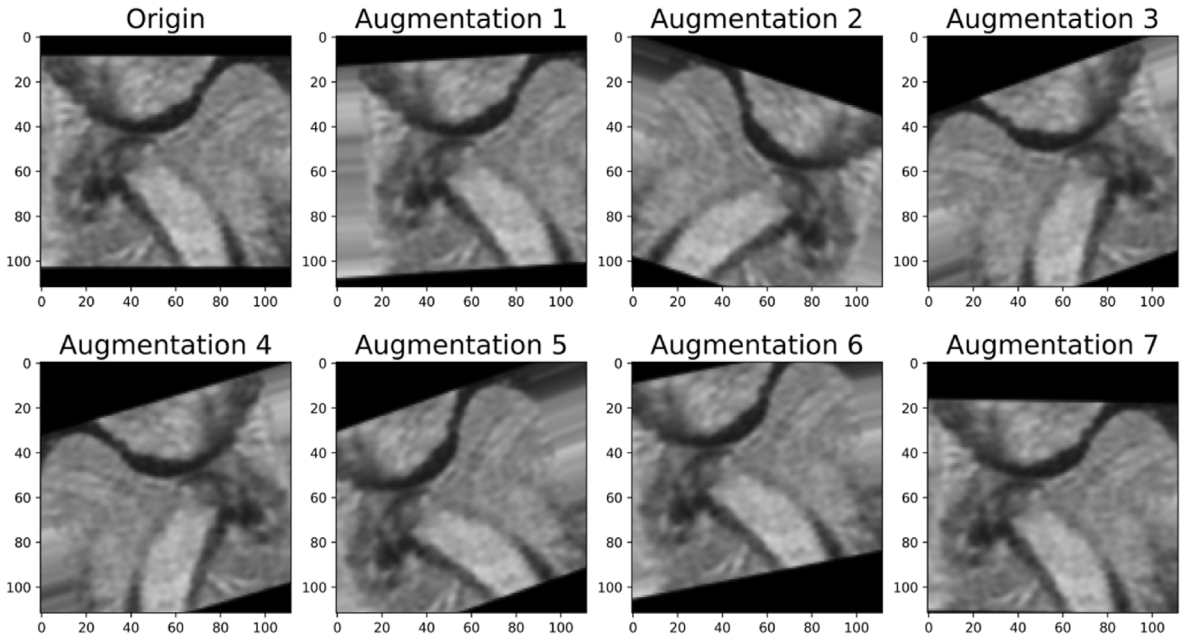

Figure 6 Data augmentation result. This figure presents the outcomes of data augmentation, where the image dataset has been expanded eightfold through random rotation and translation techniques. The augmented images demonstrate the increased diversity and variety achieved through this process.

basis. Each subject contributed multiple images, and we calculated the average of the predicted probability values from these images to obtain the predicted probability value for that subject. The resulting prediction confusion matrix is provided in Table 3. For the six-class model, the prediction accuracy was determined to be 0.8473.

Discussion

This study leveraged MRI images, which offer superior visualization of the temporal bone and mandibular condyle compared to previous use of computed tomography.[20] We developed an advanced TMJD automatic classification model powered by deep learning artificial intelligence, notable for its independence from large image databases.

Our approach included both a YOLO object detection model, enhancing the extraction of articular disc cartilage regions and noise reduction compared to prior studies,[21] and a convolutional neural network classifier capable of distinguishing patients by the severity stage of intervertebral disc displacement. The model's performance in imaging diagnosis demonstrated comparability with that of medical experts possessing extensive clinical experience.

The CNN model introduced in this study employs a human-like learning approach, interpreting the probabilities of different TMJ stages based on the expertise of oral surgery specialists. This model enables simultaneous classification into all six TMJ stages, streamlining image interpretation and enhancing prediction accuracy, achieving an impressive accuracy rate of 84.73%.

In contrast to previous applications of CNN models for TMJ image recognition, which often focused on binary classification of disease presence or absence with the highest reported accuracy of 85%,[22] our innovation lies in predicting distinct TMJ stages. Our model achieves prediction accuracies for each stage, namely 91.30%, 83.33%, 94.87%, 82.14%, and 60%, marking a significant advancement.

Moving forward, we plan to establish a feedback system where physicians can reference the CNN model's predictions. This system will exclusively provide images and TMJ stage information, respecting patient privacy. Diagnostic results from physicians will be used to fine-tune the CNN model, thereby improving its accuracy.

One notable limitation of our research lies in the relatively small number of available images. Despite our efforts to augment the dataset and increase diversity, the limited

Table 1 Data proportion. This visual representation illustrates the distribution of data proportions for each temporomandibular joint disorders (TMJD) stage,[a] including the division into training and test sets with similar proportions. Additionally, the training set is further divided into five equal parts for cross-validation. It's important to note that calculations for the left and right ears are performed independently, and the unit used is the number of subjects.

Stage	Normal	I	II	III	IV	V	Total
Train	14	43	44	68	57	17	243
Test	7	23	24	39	28	10	131

[a] The normal stage is healthy. The I stage causes a subtle sound when opening the mouth, which is usually undetectable. The II stage is the inflammatory stage. Dislocation of cartilage can be seen on imaging, causing pain in inflammatory diseases. In the III stage, although the inflammation subsides, changes in the shape of the cartilage can be seen in images. In the IV stage, the pain shifts to the muscles over the temporomandibular joint. In the V stage, the pain extends to the head and affects daily life, requiring immediate surgery.

Figure 7 VGG16 architecture. This figure illustrates the VGG16 architecture with additional modifications. It includes the incorporation of a fully connected layer with 256 units, a dropout rate of 0.1 to mitigate over-fitting, and an output layer with 6 units. These changes are made to enhance the model's performance in classifying temporomandibular joint disorders (TMJD) stages.

Table 2 Hyper-parameter grid search. This figure depicts the results of the hyper-parameter grid search, specifically focusing on the 'Freezing Layers' parameter. 'Freezing Layers' indicates the number of layers frozen from the top of the model, where the weights of the frozen layers retain their pre-training values, while the weights of the remaining unfrozen layers are iteratively updated during model training. This grid search aids in optimizing the model's performance by selecting the most suitable configuration.

Freezing layers	Mean accuracy	Mean value ± 1 standard deviation	Freezing layers	Mean accuracy	Mean value ± 1 standard deviation
0	0.7251	0.6856–0.7647	10	0.7129	0.6800–0.7459
1	0.7362	0.6936–0.7788	11	0.6957	0.6605–0.7309
3	0.7408	0.6926–0.7890	12	0.6924	0.6594–0.7254
4	0.7405	0.6933–0.7877	14	0.6578	0.5990–0.7167
6	0.7285	0.6796–0.7774	15	0.6303	0.5890–0.6717
7	0.7291	0.6991–0.7592	16	0.5775	0.5265–0.6285
8	0.7147	0.6787–0.7508	18	0.4682	0.4472–0.4893

image pool can potentially impact model accuracy. To address this challenge, we plan to establish collaborations with other affiliated hospitals to obtain MRI images from similar medical equipment, ensuring uniform image specifications through standardized preprocessing techniques.

In future research, we aim to prioritize cross-hospital collaborations to significantly expand our model's sample size and enhance its predictive capabilities. The resulting model will be made available to other hospitals for external validation, fostering broader applicability and robustness.

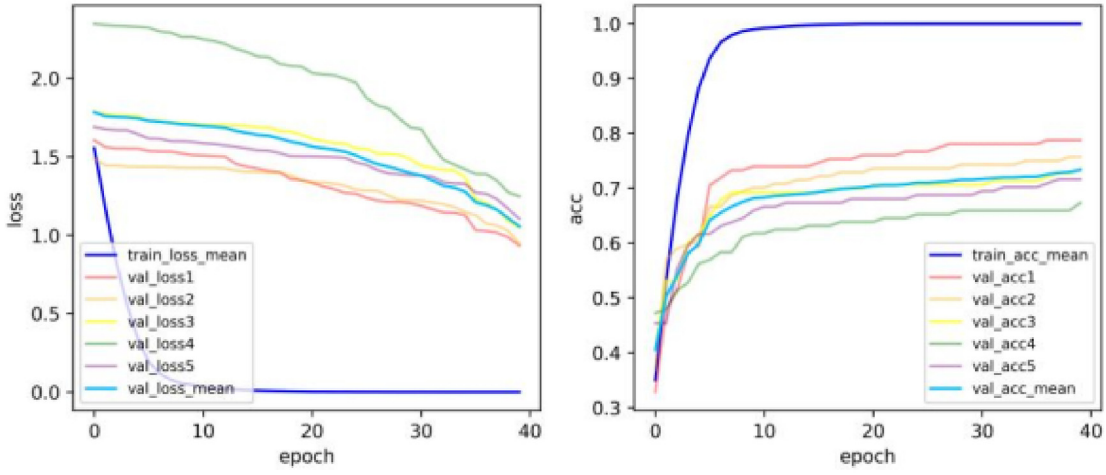

Figure 8 Iteration process curves for cross-validation. This composite figure displays the iteration process curves for cross-validation, including five loss curves and five accuracy curves representing different cross-validation folds. The average curve of the training set is highlighted in dark blue. These curves provide insights into the model's training progress and performance across multiple folds of the data. (For interpretation of the references to color in this figure legend, the reader is referred to the Web version of this article.)

Table 3 Testing confusion matrix. This matrix illustrates the testing confusion matrix, where the vertical axis represents the actual number of people, and the horizontal axis represents the predicted number of people. It provides a visual representation of the model's performance in classifying temporomandibular joint disorders (TMJD) stages and aids in assessing its accuracy.[a]

		Actual					
		Normal	Stage I	Stage II	Stage III	Stage IV	Stage V
Predicted	**Normal**	4	0	1	0	0	1
	Stage I	0	21	1	0	1	1
	Stage II	3	2	20	0	1	0
	Stage III	0	0	1	37	3	1
	Stage IV	0	0	1	2	23	1
	Stage V	0	0	0	0	0	6

[a] The normal stage is healthy. The I stage causes a subtle sound when opening the mouth, which is usually undetectable. The II stage is the inflammatory stage. Dislocation of cartilage can be seen on imaging, causing pain in inflammatory diseases. In the III stage, although the inflammation subsides, changes in the shape of the cartilage can be seen in images. In the IV stage, the pain shifts to the muscles over the temporomandibular joint. In the V stage, the pain extends to the head and affects daily life, requiring immediate surgery.

This enables cross-institution or cross-device testing to verify the generalization ability of the model.

In this study, we successfully established an automatic classification model using deep learning convolutional neural networks. Our model's capability to simultaneously diagnose multiple stages of TMJD surpasses that of previous studies, achieving an impressive accuracy rate of 84.73%. With this developed model, the automatic staging of TMJD using MRI images can serve as a valuable tool in daily clinical diagnosis and treatment planning. We anticipate further improvements in its performance through future studies, aiming to facilitate clinical practice across various institutes.

Declaration of competing interest

The authors have no conflicts of interest relevant to this article.

Acknowledgments

This work received funding from various sources, including the National Science and Technology Council (Grants: 110-2811-M-A49-550-MY2, 112-2811-M-A49-557-, 110-2118-M-A49-002-MY3, 111-2634-F-A49-014-, 112-2634-F-A49-003-, 113-2923-M-A49-004-MY3, 112-2221-E-A49-033-, 111-2314-B-075-019-, 112-2314-B-075-060-), the Taipei Veterans General Hospital (Grant: V112C-176), the Yin Shu-Tien Foundation Taipei Veterans General Hospital-National Yang Ming Chiao Tung University Excellent Physician Scientists Cultivation Program (Grant: 113-V-B-001), the Co-creation Platform of the Industry Academia Innovation School, NYCU, the Higher Education Sprout Project of the National Yang Ming Chiao Tung University from the Ministry of Education, and the Yushan Scholar Program of the Ministry of Education, Taiwan. We also thank Wan-Yi Tai for her valuable assistance and acknowledge the National Center for High-performance Computing for providing computing resources.

References

1. Ottria L, Candotto V, Guzzo F, Gargari M, Barlattani A. Temporomandibular joint and related structures: anatomical and histological aspects. *J Biol Regul Homeost Agents* 2018;32:203—7.
2. Lopes S, Costa A, Cruz A, Li L, De Almeida S. Clinical and mri investigation of temporomandibular joint in major depressed patients. *Dentomaxillofacial Radiol* 2012;41:316—22.
3. Cai XY, Jin JM, Yang C. Changes in disc position, disc length, and condylar height in the temporomandibular joint with anterior disc displacement: a longitudinal retrospective magnetic resonance imaging study. *J Oral Maxillofac Surg* 2011;69:e340—6.
4. De Rossi SS, Greenberg MS, Liu F, Steinkeler A. Temporomandibular disorders: evaluation and management. *Med Clin* 2014;98:1353—84.
5. Talaat WM, Adel OI, Al Bayatti S. Prevalence of temporomandibular disorders discovered incidentally during routine dental examination using the research diagnostic criteria for temporomandibular disorders. *Oral Surg Oral Med Oral Pathol Oral Radiol* 2018;125:250—9.
6. Racich MJ. Occlusion, temporomandibular disorders, and orofacial pain: an evidence-based overview and update with recommendations. *J Prosthet Dent* 2018;120:678—85.
7. Ferreira LA, Grossmann E, Januzzi E, Mvqd Paula, Carvalho ACP. Diagnosis of temporomandibular joint disorders: indication of imaging exams. *Braz J Otorhinolaryngol* 2016;82:341—52.
8. Lee YH, Won JH, Kim S, Auh QS, Noh YK. Advantages of deep learning with convolutional neural network in detecting disc displacement of the temporomandibular joint in magnetic resonance imaging. *Sci Rep* 2022;12:11352.
9. Ozsari S, Güzel MS, Yılmaz D, Kamburoğlu K. A comprehensive review of artificial intelligence based algorithms regarding temporomandibular joint related diseases. *Diagnostics* 2023;13:2700.
10. Rehman A, Saba T. Neural networks for document image preprocessing: state of the art. *Artif Intell Rev* 2014;42:253—73.
11. Takahashi R, Matsubara T, Uehara K. Data augmentation using random image cropping and patching for deep cnns. *IEEE Trans Circ Syst Video Technol* 2019;30:2917—31.
12. Jeong H-J, Park K-S, Ha Y-G. Image preprocessing for efficient training of yolo deep learning networks. In: *Proceedings from*

the 2018 IEEE International conference on big data and smart computing (BigComp); 2018.
13. Du J. Understanding of object detection based on cnn family and yolo. In: *Proceedings from the journal of physics: conference series*; 2018.
14. Redmon J, Farhadi A. *Yolov3: an incremental improvement*. 2018. *arXiv preprint arXiv:1804.02767*.
15. Hashemi M. Enlarging smaller images before inputting into convolutional neural network: zero-padding vs. interpolation. *J Big Data* 2019;6:1—13.
16. Wang Q, Yuan Y. Learning to resize image. *Neurocomputing* 2014;131:357—67.
17. Anwar S, Tahir M, Li C, Mian A, Khan FS, Muzaffar AW. *Image colorization: a survey and dataset*. 2020. *arXiv preprint arXiv: 2008.10774*.
18. Humayun AI, Ghaffarzadegan S, Feng Z, Hasan T. Learning front-end filter-bank parameters using convolutional neural networks for abnormal heart sound detection. In: *Proceedings from the 2018 40th annual international conference of the IEEE engineering in medicine and biology society*. EMBC), 2018.
19. Tsamardinos I, Rakhshani A, Lagani V. Performance-estimation properties of cross-validation-based protocols with simultaneous hyper-parameter optimization. *Int J Artif Intell Tool* 2015;24:1540023.
20. Choi E, Kim D, Lee JY, Park HK. Artificial intelligence in detecting temporomandibular joint osteoarthritis on orthopantomogram. *Sci Rep* 2021;11:10246.
21. Nozawa M, Ito H, Ariji Y, et al. Automatic segmentation of the temporomandibular joint disc on magnetic resonance images using a deep learning technique. *Dentomaxillofacial Radiol* 2022;51:20210185.
22. Kao ZK, Chiu NT, Wu HTH, et al. Classifying temporomandibular disorder with artificial intelligent architecture using magnetic resonance imaging. *Ann Biomed Eng* 2023;51:517—26.